Reactivity of halogens on a Si(111) surface studied by surface differential reflectivity

M. Tanaka,* E. Yamakawa,† T. Shirao,‡ and K. Shudo
Department of Physics, Faculty of Engineering, Yokohama National University, 79-5 Tokiwadai, Hodogaya-ku, Yokohama 240-8501, Japan

(Received 15 April 2003; revised manuscript received 15 August 2003; published 20 October 2003)

The adsorption of Br on a Si(111)7×7 surface at room temperature and the isothermal desorption of silicon bromides from a Br-terminated Si(111) rest atom surface at about 900 K have been investigated by means of *in situ* real-time surface differential reflectivity (SDR) spectroscopy in order to elucidate the fundamental processes of Br-etching. The present results are compared with those of previous SDR studies on chlorine adsorption and chloride desorption. In the adsorption process, both the sticking probability on adatom dangling bonds and the breaking probability of adatom back bonds are larger than those for Cl adsorption. In the desorption process, the activation energy for bromide desorption (1.8 eV) is smaller than that for chloride desorption. The experimental results can be well interpreted in terms of larger repulsive interaction between Br adsorbates. The activation energy for the formation of the dimer-adatom-stacking fault structure (3.5 eV) is larger than that for the surface after chloride desorption.

DOI: 10.1103/PhysRevB.68.165411 PACS number(s): 68.43.Mn, 68.47.Fg, 78.68.+m, 68.43.Vx

I. INTRODUCTION

Etching with halogen gases is widely used in semiconductor technology, and is a promising candidate method for layer-by-layer etching, which is one of the basic techniques to fabricate nanometer-scale structures. Halogen etching consists of several stages: adsorption of halogen atoms on the surface, desorption of silicon halides, and reconstruction of the clean surface. An understanding of the atomic scale mechanisms of these fundamental processes will be useful to optimize etching conditions. Etching of the Si(100) surface is preferentially studied in connection with industrial applications, but etching of the Si(111) surface is also of interest, because the dimer-adatom-stacking fault (DAS) structure has a variety of sites with different chemical reactivities.[1] Different halogens will react with a semiconductor surface in different ways, because they have different ionic radii and different electron affinities. Understanding the chemical trend of halogen reactivity is crucial to optimize etching conditions. On Si(100), several studies have proved the existence of a repulsive interaction between adsorbates for larger halogens (Br and I), in terms of the presence of stable $c(4\times2)$ structure and lower desorption energy.[2–6] However, there is no such study on Si(111), and in fact, similarity among Cl-, Br-, and I- terminated 1×1 structures was reported.[7] Are the fundamental processes of Br etching of Si(111) similar to those of Cl etching? That is the question we would like to answer in this study.

The static properties at each stage in the fundamental processes of halogen etching have been revealed by a variety of methods. It is known that chlorine atoms first react with adatom sites to form monochlorides and remove dangling bond states near low coverage,[8,9] while further exposure produces $SiCl_2$ and $SiCl_3$ species.[10,11] On the other hand, there is little direct evidence for the presence of polybromide species, although their presence is generally accepted. Annealing at about 700 K for a Cl-covered surface and at 500–650 K for a Br-covered surface removes Si adatoms, and the rest atom surface covered with Br atoms takes a 1×1 structure.[9,12] Many bilayer islands and clusters are found on the 1×1 Br-terminated rest atom surface.[12,13] Polybromide species are desorbed at about 600 K, and monobromide species are desorbed above 900 K as $SiBr_2$.[14] As for the desorption mechanism, a scanning tunneling microscope study indicated that spontaneous Br etching of Si(111) at 700–900 K results in step retreat.[12] A surface differential reflectivity spectroscopy (SDR) study on chloride desorption suggested that the desorption from clusters proceeds together with the desorption from steps.[15] Thus, the dynamic process at each stage of bromine-etching of Si(111) has not yet been fully understood, and needs to be established before the relative reactivity of halogens on the Si(111) surface can be discussed.

Real-time observation is essential to investigate kinetics. Optical methods are superior to others, because they are noninvasive, nondestructive, and capable of very rapid response. SDR is a powerful tool to study adsorption processes in real time.[16] Differential reflectivity is defined as $\Delta R/R=(R_a-R_c)/R_c$, where R_a and R_c are the reflectivities of the adsorbed and the clean surfaces, respectively. Spectral features of adsorption on adatom dangling bonds and breaking of adatom back bonds were identified from the calculation of the $\Delta R/R$ spectrum for the hydrogenated 7×7 surface.[17] The adsorption process of chlorine on Si(111)7×7 was elucidated by the same method.[18] SDR is also a powerful tool to investigate the desorption process by monitoring the recovery of dangling bonds and back bonds during chloride desorption from a Cl-terminated Si(111) rest atom surface.[15]

In the present study, the adsorption process of bromine on a Si(111)7×7 surface and the desorption process of silicon bromide from a Br-terminated Si(111) rest atom surface were investigated in real time by means of SDR. One should note that the structure of the rest atom surface on which the desorption takes place is different from the 7×7 DAS structure on which the adsorption takes place. The Br adsorption process has been investigated at room temperature, while the bromide desorption process and subsequent restoration of the DAS structure have been investigated between 873 and 923 K. The time courses of the disappearance of the dangling

bonds and the back bonds yield the rate constants in the adsorption process, whereas the time courses of their recovery yield the rate constants, the order of reaction, and the activation energies in the desorption process. The kinetics of the adsorption and desorption and restoration processes are evaluated here from the bond density data. They are compared with the results of previous SDR studies on Cl adsorption and chloride desorption on Si(111),[15,18] and the difference in the reactivity of bromine and chlorine on Si(111) is discussed in terms of the interaction between adsorbates.

II. EXPERIMENT

Measurements were performed in an ultrahigh vacuum chamber at a base pressure of 2×10^{-8} Pa. A specimen of $5\times18\times0.38$ mm^3 was cut from a B-doped *p*-type Si(111) wafer (10–15Ω cm). The specimen was ohmically heated to 1470 K for several seconds and slowly cooled to obtain the 7×7 DAS structure. The 7×7 structure was confirmed by low-energy electron diffraction. Br gas was generated with a AgBr electrochemical cell doped with $CdBr_2$ (5 wt %).[19] The electrochemical cell produces more atoms than molecules.[20] Actually, any trace of Br_2 species was not observed with a quadrupole mass spectrometer during the Br gas exposure. The cell outlet was directed to the surface of the specimen, so that incident flux of Br atoms onto the surface was much larger than that in the case of back filling. This flux was estimated from the output of the vacuum gauge, using the pumping speed and the area of the specimen.

In the isothermal desorption measurement, the Br-saturated surface was annealed at 673 K for 3 min in order to desorb polybromide species and to form the rest atom surface. Otherwise the desorption of both polybromide and monobromide species would proceed at the same time in isothermal desorption at higher temperatures. After the annealing at 673 K, isothermal desorption of silicon bromides from the rest atom surface was observed by SDR between 873 and 923 K.

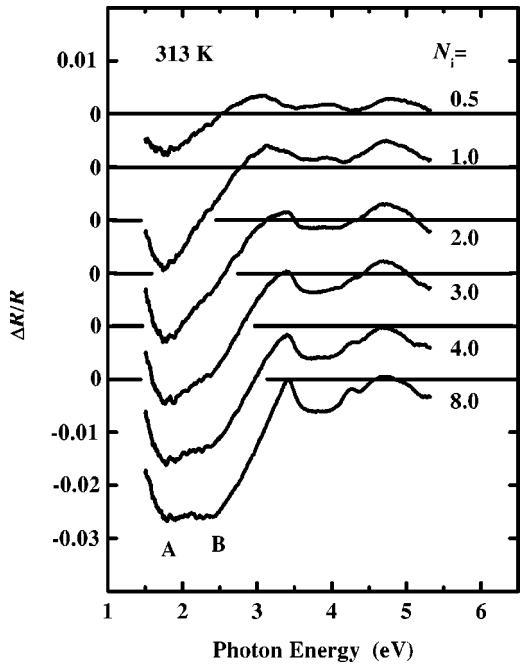

FIG. 1. Variation of *p*-polarized reflectance spectra during Br adsorption at 313 K. N_i is the number of atoms impinging on the area of the 1×1 unit cell. The feature *A* originating from the dangling bonds develops first, the feature *B* from the back bonds appears later.

The temperature was monitored with an electronic pyrometer. The experimental setup for SDR has been described in detail elsewhere.[18] Light from a halogen tungsten lamp or a deuterium lamp was polarized horizontally and separated into a probe beam (90%) and a reference beam (10%). The *p*-polarized probe beam was introduced into the vacuum chamber and was incident on the surface at an angle of 70° from the surface normal. The specularly reflected probe beam and the reference beam were introduced via optical fibers to a grating spectrograph. The spectra of both beams were detected by a dual photodiode array, and the intensity of the reflected spectrum was normalized with respect to the reference spectrum. Photoinduced electrons in the diode array were accumulated at each pixel for 20 s to improve the signal-to-noise ratio. At each temperature, spectrum of a clean surface R_c and that of a Br-covered surface R_a were measured in that order to obtain a differential reflectivity spectrum $\Delta R/R=(R_a-R_c)/R_c$.

III. RESULTS AND DISCUSSION

A. Adsorption of halogen gas

Figure 1 shows the SDR spectra in the visible and ultraviolet ranges for several Br exposures at 313 K. The exposure is represented by N_i which is the number of atoms impinging on the area of the 1×1 unit cell. The $\Delta R/R$ spectrum at $N_i=0.5$ has a negative peak *A* located at 1.8 eV. At $N_i=3.0$, a shoulder *B* at 2.4 eV is apparent. As in the case of H adsorption,[17] these features arise from the disappearance of electronic states of the clean 7×7 DAS structure. The feature *A* is ascribed to missing transitions between surface states involving adatom dangling bond states and *B* to missing transitions from adatom back bond states to bulk states. The peak energies of the features in the higher-energy range agree with those of E_1 and E_2 edges in the reflectance spectrum, and these features were ascribed to bulk states modulated due to the adsorption. The feature *A* is almost saturated at $N_i=3.0$, whereas *B* is saturated above $N_i=8.0$. The appearance of the feature *B* means that adatom back bonds are broken and polybromide species are formed. This is the first direct evidence for polybromide species formation on the Br-covered Si(111)7×7 surface. Meanwhile, adsorption on the dangling bonds of rest atoms of the DAS structure does not contribute to the SDR features, because the filled dangling bond states of rest atoms are clearly below the filled dangling bond states of adatoms.[21,22] This was demonstrated by the experiment that showed that the sticking probability determined from SDR is nearly equal to that determined from surface second-harmonic generation (SHG).[18] It is well known that SHG does not detect the dangling bond states of rest atoms.[23]

The overall features of the SDR spectra in Fig. 1 are similar to those for Cl adsorption on Si(111)7×7, and the procedure for analysis of $\Delta R/R$ is described in detail in Ref.

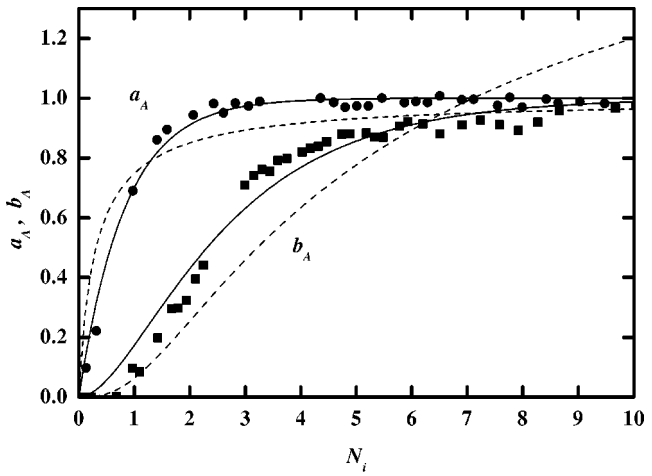

FIG. 2. Coefficients a_A (solid circles) and b_A (solid squares) vs exposure at 313 K. This reveals the development of the adsorption on the adatom dangling bonds and that of the breaking of the adatom back bonds. Solid lines are best-fit curves for direct adsorption of atoms, whereas dashed lines are for dissociative adsorption of molecules.

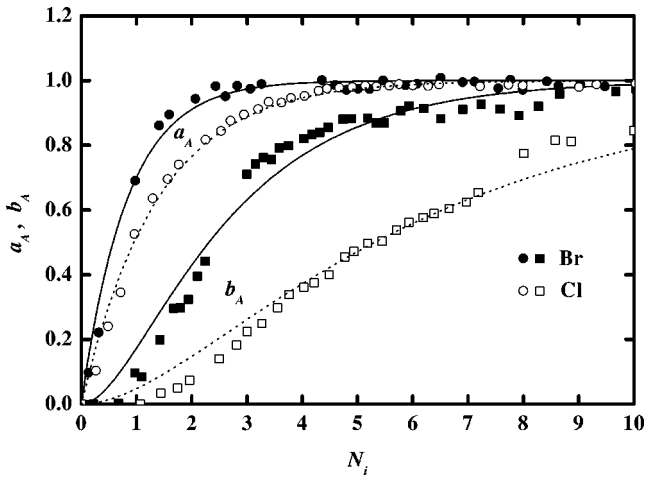

FIG. 3. Development of the coefficients a_A and b_A vs N_i at 313 K. Solid circles and squares are for Br adsorption, whereas open circles and squares are for Cl adsorption (Ref. 18). Solid and dashed lines are best-fit curves for the experimental plots of direct adsorption of atoms.

18. Each $\Delta R/R$ spectrum in Fig. 1 is reproduced by a linear combination $(a_A S_A + b_A S_B)$ of two-component spectra S_A and S_B, representing the features A and B, respectively. The magnitudes of S_A and S_B are determined so as to reproduce the saturated $\Delta R/R$ spectra at $N_i = 20.0$ with $a_A = 1$ and $b_A = 1$. As shown in Fig. 2, thus obtained a_A (solid circles) and b_A (solid squares) reveal the development of adsorption on the adatom dangling bonds and the development of breaking of the adatom back bonds, respectively. The horizontal axis corresponds to N_i.

The adsorption on adatom dangling bonds is analyzed as follows. In the case of direct adsorption of Br atoms without migration, the rate equation is as follows:

$$\frac{dn_A}{dt} = \alpha n_i (1 - n_A). \tag{1}$$

Here, n_A is the normalized density of adatoms bonded to at least one Br atom, α is the sticking probability of Br atoms on the adatom dangling bond, and n_i is the number of atoms impinging on the area of the 1×1 unit cell per second. In the case of dissociative adsorption of Br molecules which produces two adsorbates from one molecule, the rate equation is as follows:

$$\frac{dn_A}{dt} = \alpha' n_i' (1 - n_A)^2, \tag{2}$$

where α' is the sticking probability of Br molecules on the adatom dangling bond and n_i' is the number of Br molecules impinging on the area of the 1×1 unit cell per second. Solutions of Eqs. (1) and (2) fitted to a_A are shown by solid and dashed lines in Fig. 2, respectively. The solution of Eq. (1) fits much better than that of Eq. (2). Consequently, atoms are found to play an essential role in the adsorption on the adatom dangling bond. Solutions of rate equations including the migration of atoms were also calculated. However, they did not agree with the data as well as the solution of Eq. (1).

On the other hand, the breaking of the adatom back bond is analyzed as follows. The adatom back bond is assumed to be broken only when the adatom dangling bond is terminated by at least one Br atom. In the case of direct adsorption of atoms without migration, the rate equation is as follows:

$$\frac{dn_B}{dt} = \beta n_i (N_B n_A - n_B), \tag{3}$$

where β is the breaking probability of adatom back bonds, n_B is the normalized density of broken adatom back bonds, and N_B is the saturated number of n_B. N_B should be smaller than 2 because adatoms are not removed by the Br exposure. In the case of dissociative adsorption of Br molecules which produces two adsorbates from one molecule, the rate equation is as follows:

$$\frac{dn_B}{dt} = \beta' n_i' (N_B n_A - n_B)^2, \tag{4}$$

where β' is the breaking probability of adatom back bond by Br molecules. Solutions of Eqs. (3) and (4) fitted to b_A are shown by solid and dashed lines in Fig. 2, respectively. The solution of Eq. (3) fits much better than that of Eq. (4). Consequently, atoms are also found to play an essential role in the breaking of the adatom back bond.

Figure 3 compares Fig. 2 with the results for Cl adsorption. Open circles and open squares represent a_A and b_A for Cl adsorption on Si(111)7×7 at room temperature, respectively, and are well fitted by dashed lines calculated using Eqs. (1) and (3).[18] The present SDR study provides a direct evidence for back bond breaking with Br and polybromide species formation. The dynamic process of Br adsorption is also revealed. Several measurements at 313 K yield the sticking probability $\alpha = 1.20 \pm 0.2$, and the breaking probability $\beta = 0.49 \pm 0.04$, on the adatom. A value α larger than 1 is

TABLE I. Summary of SDR results for the adsorption and desorption processes of halogens on Si(111)7×7.

	Br	Cl
(1) Adsorption at room temperature		
Initial sticking probability on the adatom dangling bonds (feature *A*)	1.2±0.2	0.7 [a]
Initial breaking probability of the adatom back bonds (feature *B*)	0.49±0.04	0.2 [a]
(2) Desorption		
(a) Recovery of the dangling bonds (feature *A′*)		
Order	1st	1st [b]
Rate constant at 903 K	0.01 s^{-1}	0.008 s^{-1} [b]
Activation energy for the desorption	1.8±0.4 eV	2.3±0.3 eV [b]
(b) Recovery of the back bonds (feature *B′*)		
Order	1st	1st [b]
Rate constant at 903 K	0.003 s^{-1}	0.004 s^{-1} [b]
Activation energy for the reconstruction	3.5±0.6 eV	2.8±0.5 eV [b]

[a]Reference 18.
[b]Reference 15.

seemingly strange. However, this is reasonable if Br atoms incident outside the area of the 1×1 unit cell centered on the adatom are absorbed preferentially on the adatom. This situation is very likely because the electronic charge density of adatom dangling bonds extends widely into the vacuum.[24] On the other hand, $\alpha=0.7$ and $\beta=0.2$ were reported for Cl adsorption.[18] These results are summarized in Table I. The sticking probability α for Br adsorption is 1.7 times as large as α for Cl adsorption. Larger α for Br adsorption can be at least partially explained by the larger atomic radius of the Br atom (0.115 nm for Br and 0.100 nm for Cl),[25] because the cross section of the collision to the adatom dangling bond is larger for larger impinging atoms. However, the ratio of the atomic radius, 1.15, is smaller than the ratio of α, 1.7, so that this explanation seems insufficient. Another possibility is considered later.

The breaking probability β for Br adsorption is 2.5 times as large as β for Cl adsorption. This means that the back bond is broken more easily by Br than by Cl. In other words, polybromide species are produced more easily than polychloride species. The same chemical trend was observed in an electron-stimulated ion desorption study, which implied that the desorption of $SiBr_2^+$ ions, suggesting polybromide formation, is apparent even at coverage as low as 0.1 monolayer (ML) for the Br-covered Si(111), though no ion containing Si is detected from Cl-covered Si(111) at such low coverage.[26] At 0.1 ML, only a quarter of the dangling bonds of adatoms and rest atoms adsorb Br atoms. These results therefore suggest that a Br atom impinging close to a Br-adsorbed adatom tends to break the back bond rather than be adsorbed on the rest atom, even at a low coverage. This may be caused by the large repulsive interaction between Br adsorbates which is evident on Si(100).[2–6] The repulsive interaction between Br adsorbates may also produce a larger sticking probability for Br adsorption, because an impinging Br atom will tend to be adsorbed on an adatom rather than a rest atom due to the interaction.

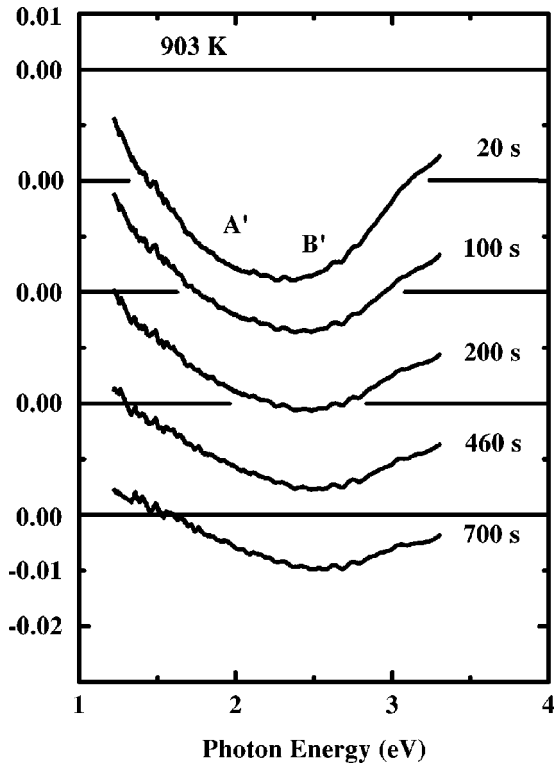

FIG. 4. Variation of *p*-polarized reflectance spectra during isothermal desorption at 903 K. The feature *A* originating from the adatom dangling bonds decays first, and the feature *B* from the back bonds remains even at 700 s. Note that the energy scale of the horizontal axis is enlarged from Fig. 1.

B. Desorption of silicon halides

Figure 4 shows the SDR spectra in the visible and infrared ranges during isothermal desorption at 903 K. Here, $\Delta R/R=(R_a-R_c)/R_c$, and both R_a and R_c were measured at 903 K. The spectra were measured in the range from 1.18 to 3.3 eV, because the feature A' spreads over the infrared range at 903 K and the main part of the feature B' appears below 3.0 eV. The spectrum at 20 s has seemingly a single negative peak at around 2.3 eV. However, the band shape changes with time, and only a negative peak at 2.5 eV remains at 460 s. Therefore, the spectrum at 20 s should be considered as the combination of negative peaks A' at around 1.7 eV and B' at around 2.4 eV. The feature A' is depressed faster than B', and almost disappears at 460 s, whereas B' remains even at 700 s. These spectral features are quite similar to those observed for adsorption at room temperature (Fig. 1) except for broadening of spectral features due to high temperature. The

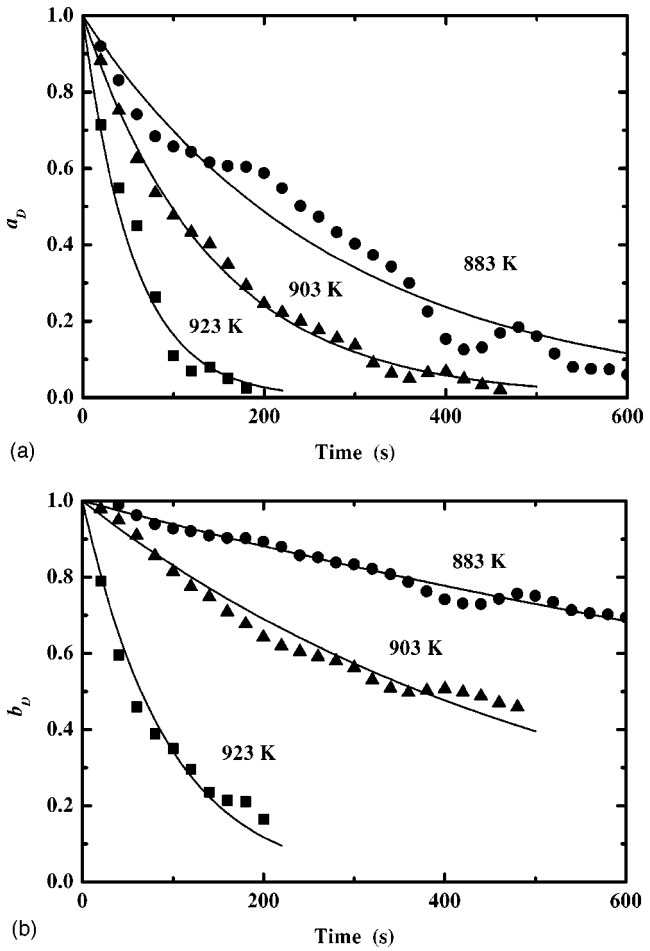

FIG. 5. Time courses of the coefficients (a) a_D and (b) b_D at 873 K (solid circles), 903 K (solid triangles), and 933 K (solid squares). This reveals the recovery of the dangling bonds (a) and the adatom back bonds (b). Solid lines are best-fit curves obtained by using first-order kinetics.

decay of these features therefore corresponds to the restoration of the structure of the clean surface.

The overall features of the SDR spectra in Fig. 4 are similar to those for chloride desorption from the Si(111) rest atom surface, and the procedure for analysis of $\Delta R/R$ is described in detail in Ref. 15. Each $\Delta R/R$ spectrum in Fig. 4 is reproduced by a linear combination ($a_D S_A + b_D S_B$) of the two-component spectra S_A and S_B representing the features A' and B', respectively. The values a_D and b_D at several temperatures are plotted in Figs. 5(a) and 5(b), respectively, which illustrate the recovery of the dangling bonds and the back bonds. They are normalized so that the value fitted by Eq. (5) described below is unity at 0 s. When the first-order process is dominant, the decay is expressed with a rate constant κ,

$$x(t) = e^{-\kappa t}, \tag{5}$$

where x stands for a_D or b_D. The solid lines in Fig. 5 are best-fit curves obtained by using Eq. (5). These curves well reproduce the overall features of the decay of a_D and b_D. The fit with higher order was worse than the fit with first

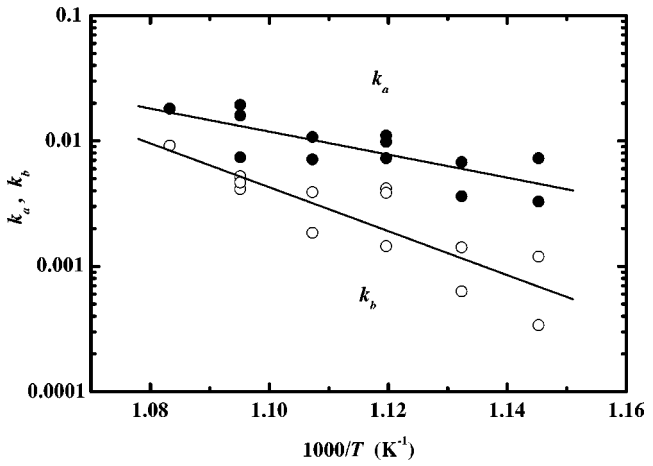

FIG. 6. Logarithmic plots of the decay rates κ_a (solid circles) and κ_b (open circles). Solid lines are best linear fits to the plots, giving the activation energies $E_a = 1.8 \pm 0.4$ eV and $E_b = 3.5 \pm 0.6$ eV.

order, indicating that these processes are dominated by first-order kinetics. The decay constant κ for the recovery rate of the dangling bond, κ_a, and that for the recovery rate of the back bond, κ_b, are determined by these fits at each temperature. In the case of a thermally activated process, the temperature dependence of κ is expressed with an activation energy E_d:

$$\kappa = \kappa^0 \exp\left[-\frac{E_d}{k_B T}\right]. \tag{6}$$

The temperature dependences of the obtained κ_a and κ_b are shown in Fig. 6 with solid and open circles, respectively. The solid lines are the best linear fits to the plots. The activation energies in the recovery process of the dangling bonds and the back bonds are determined as $E_a = 1.8 \pm 0.4$ eV and $E_b = 3.5 \pm 0.6$ eV, respectively. These results are summarized in Table I and compared with the results for chloride desorption from Si(111).[15] The order of the process, the rate constant at 903 K and the activation energy are listed.

1. Recovery of the dangling bond

After the annealing at 673 K for 3 min, all polybromides including Si adatoms are desorbed[14] and the adatom layer disappears.[12,13] Instead, the Br-terminated rest atom surface appears together with clusters including brominated adatoms.[12,13] Thus, at about 900 K, silicon bromides are considered to be desorbed from two sources. One is monobromides on the rest atom surface and the other is monobromides or polybromides on the culster surface.

The result for the feature A' agrees well with that in the case of chloride desorption, except for the activation energies, indicating that the desorption mechanism of silicon bromide is similar to that of the chloride[15] as summarized below. The faster recovery of the dangling bonds (feature A') compared with the recovery of the back bonds (feature B') is interpreted as indicating that the feature A' can decay before the adatom is restored. This is because a dangling bond on

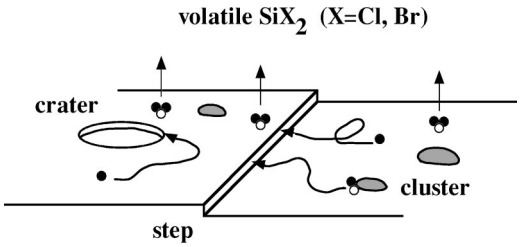

FIG. 7. Schematic view of the proposed desorption mechanism. There are two types of desorption: desorption from defects on the rest atom surface, such as steps and craters, and desorption from clusters.

the rest atom surface makes nearly the same contribution to the $\Delta R/R$ spectrum as that of the adatom on the DAS surface. Actually, the energy of the dangling bond states on the rest atom surface was calculated to be $E_F \pm 0.5$ eV.[28] In comparison with the dangling bond states of adatoms on the 7×7 DAS surface,[29] the difference in the peak energy of the feature A is estimated to be much smaller than its bandwidth.[16] Thus, the peak energy difference between the rest atom surface and the DAS surface affects the feature A only slightly. On the other hand, contribution from the dangling bond on the cluster can be negligible for the following two reasons. The area of the cluster surface is much smaller than that of the rest atom surface and the dangling bond states on the cluster can be well separated from those on the DAS surface. Consequently, the decay of the feature A' is considered to represent the desorption of silicon bromides from the Br-terminated rest atom surface, and the activation energy for the feature A' corresponds to the desorption energy. The thermal desorption specrotoscopy (TDS) study of bromide desorption from Si(111) (Ref. 14) indicates that $SiBr_2$ is the main desorption species at around 900 K. Judging from the first-order kinetics and the activation energy in Table I, the recombinative desorption of $SiBr_2$ from the ideal terrace of the Br-terminated rest atom surface is unlikely, and defects such as steps and craters are thought to play an important role in the desorption process.[12] The desorption from these defects can follow first-order kinetics because of its one dimensionality. In the case that the Br density at the defect is proportional to the Br density on the rest atom surface, which is established under thermal equilibrium, the dangling bond density detected by SDR seems to increase following first-order kinetics. This desorption model is schematically illustrated in Fig. 7. Other surface-sensitive methods to detect the dangling bond density (SHG) (Ref. 27) and the Cl density (ultraviolet photoelectron spectroscopy),[30] which are insensitive to the desorption from the cluster, also see first-order kinetics for the chloride desorption. On the other hand, methods detecting species desorbed from both the rest atom layer and the cluster, such as temperature-programmed desorption,[14,31] laser-induced thermal desorption,[32] and steady-state etching,[33] see second-order kinetics. This discrepancy has been explained by the model that the desorption from the cluster with larger activation energy lasts longer than that from the defect.[15]

According to the above desorption model, the activation energy of 1.8 eV is ascribed to the energy required to form a volatile $SiBr_2$ molecule at the defects, because the energy barrier for Br and $SiBr_x$ diffusion is presumed to be low. The present activation energy is smaller than that for the chloride desorption, 2.3 eV.[15] The local structure of the dimer at the step edge on Si(111) is similar to that of the dimer on Si(100).[12] The energy for bromide and chloride desorption on Si(100) can therefore be taken into consideration in discussing the desorption energy on Si(111). According to *ab initio* electronic structure calculation on Si(100),[2] the desorption energy for $SiBr_2$ (2.31 eV) is smaller than that for $SiCl_2$ (3.11 eV). The smaller desorption energy of $SiBr_2$ was assigned mainly to the larger strain due to the repulsive interaction between monobromide species and not due to a decrease in the bond charge. On the other hand, TDS studies of bromide and chloride desorption from Si(100) showed that the activation energy for $SiBr_2$ is 1.9 eV and that for $SiCl_2$ is 2.4 eV.[34,35] The activation energies on Si(100) are quite similar to our results on Si(111), so that the smaller activation energy for $SiBr_2$ on Si(111) can also be assigned to the larger strain due to the repulsive interaction between Br adsorbates.

2. Recovery of the adatom back bond

The result for the feature B' in Table I agrees well with that in the case of chloride desorption, except for the activation energies, indicating that the DAS formation mechanism is similar to that of the surface after chloride desorption.[15] Dangling bonds appear on the rest atom surface as $SiBr_2$ molecules are desorbed, and adatom back bonds subsequently recover. Since the energy required for the diffusion of Si clusters is estimated to be lower than 1.5 eV,[36,37] the activation energy for the feature B' corresponds to the structural change. The feature B' does not decay when the adatom only sits on the T_4 site, but it decays later when the stacking fault structure is formed. Various $n\times n$ DAS structures have been found during reconstruction from the quenched 1×1 phase, and the 7×7 DAS structure is formed through a size change process.[38,39] However, SDR cannot distinguish the 7×7 DAS structure from other $n\times n$ DAS structures ($n=3,5,9,11$, and so on) because of the large bandwidth of spectral features.[15]

The activation energy for recovery of the back bond was found to be 3.5 ± 0.6 eV. Although the DAS structure consists of several elements, such as dimers, a corner hole, and stacking faults, these elements are inherently inseparable.[38] Accordingly, the obtained activation energy should be compared with the formation energy for a faulted half unit cell, which is reported as 2.6 eV.[36] This value is close to the activation energy for the surface after chloride desorption,[15] but meaningfully smaller than that for the surface after bromide desorption. Accordingly, additional mechanisms giving higher activation energy should be taken into account for the surface after bromide desorption. Although the nature of such a mechanism cannot be determined from the SDR results, surface morphology could affect the process of DAS structure formation, as pointed out in Ref. 40.

IV. SUMMARY

Three fundamental processes of Br etching of the Si(111) surface have been investigated by means of *in situ* real-time

SDR spectroscopy. They are adsorption of bromine on a Si(111)7×7 surface, isothermal desorption of silicon bromides from a Br-teminated Si(111) rest atom surface, and subsequent restoration of the DAS structure. The spectral features A (A') and B (B') arise mainly from missing adatom dangling bonds and missing adatom back bonds of the DAS structure, respectively. Time courses of the disappearance of the dangling bonds and the back bonds in the adsorption process and those of their recovery in the desorption process are determined from the magnitudes of the corresponding spectral features. From the time courses, the rate constants of the adsorption process, and the rate constants, the order of reaction and the activation energies of the desorption process are obtained.

The present results were compared with the previous SDR studies on Cl adsorption and chloride desorption on Si(111).[15,18] The mechanisms of the adsorption and desorption and restoration processes were found to be qualitatively the same for Br and Cl, but quantitatively different. In the adsorption process of Br, both the sticking probability on dangling bonds and the breaking probability of back bonds are larger than those for Cl adsorption. In the desorption process, the activation energy for bromide desorption (1.8 eV) is smaller than that for chloride desorption. This chemical trend is interpreted in terms of larger strain due to repulsive interaction between Br adsorbates. The activation energy for the dimer-adatom-stacking fault (DAS) structure formation (3.5 eV) is larger than that for the surface after chloride desorption.

This study has revealed the chemical trend of halogen reactivity on the Si(111) surface, which should be a useful information to optimize etching conditions, as well as to improve our understanding of the fundamental processes in the halogen etching of Si surfaces. Our results suggest that Br etching is superior to Cl etching, because the smaller desorption energy means better controllability of the etching process, and the larger interaction between adsorbates may be used for site-selective etching.

*Electronic address: mtanaka@ynu.ac.jp
†Present address: Technology Operations Systems, Merrill Lynch Japan Securities Co., Ltd., 1-1-3 Otemachi, Chiyoda-ku, Tokyo 100-8180, Japan.
‡Present address: Ulvac-Phi, Inc., 370 Enzo, Chigasaki, Kanagawa 253-0084, Japan.

[1] C.M. Aldao and J.H. Weaver, Prog. Surf. Sci. **68**, 189 (2001).
[2] H. Aizawa, S. Tsuneyuki, and T. Ogitsu, Surf. Sci. **438**, 18 (1999).
[3] C.F. Hermann and J.J. Boland, Surf. Sci. **460**, 223 (2000).
[4] K. Nakayama, C.M. Aldao, and J.H. Weaver, Phys. Rev. B **59**, 15 893 (1999).
[5] D. Rioux, F. Stepniak, R.J. Pechman, and J.H. Weaver, Phys. Rev. B **51**, 10 981 (1995).
[6] G.A. de Wijs and A. Selloni, Phys. Rev. B **64**, 041402 (2001).
[7] B.S. Itchkawitz, M.T. McEllistrem, and J.J. Boland, Phys. Rev. Lett. **78**, 98 (1997).
[8] J.S. Villarrubia and J.J. Boland, Phys. Rev. Lett. **63**, 306 (1989).
[9] J.J. Boland and J.S. Villarrubia, Phys. Rev. B **41**, 9865 (1990).
[10] R.D. Schnell, D. Rieger, A. Bogen, F.J. Himpsel, K. Wandelt, and W. Steinmann, Phys. Rev. B **32**, 8057 (1985).
[11] L.J. Whitman, S.A. Joyce, J.A. Yarmoff, F.R. McFeely, and L.J. Terminello, Surf. Sci. **232**, 297 (1990).
[12] R.J. Pechman, X.-S. Wang, and J.H. Weaver, Phys. Rev. B **52**, 11 412 (1995).
[13] H. Grub and J.J. Boland, Surf. Sci. **407**, 152 (1998).
[14] T. Shirao, K. Shudo, Y. Tanaka, T. Nakajima, T. Ishikawa, and M. Tanaka, Jpn. J. Appl. Phys., Part 1 **42**, 593 (2003).
[15] M. Tanaka, S. Minami, K. Shudo, and E. Yamakawa, Surf. Sci. **527**, 21 (2003).
[16] C. Beitia, W. Preyss, R. Del Sole, and Y. Borensztein, Phys. Rev. B **56**, R4371 (1997).
[17] C. Noguez, C. Beitia, W. Preyss, A.I. Shkrebtii, M. Roy, Y. Borensztein, and R. Del Sole, Phys. Rev. Lett. **76**, 4923 (1996).
[18] M. Tanaka, T. Shirao, T. Sasaki, K. Shudo, H. Washio, and N. Kaneko, J. Vac. Sci. Technol. A **20**, 1358 (2002).
[19] N.D. Spencer, P.J. Goddard, P.W. Dacies, M. Kitson, and R.M. Lambert, J. Vac. Sci. Technol. A **1**, 1554 (1983).
[20] M. Suguri, Ph.D. thesis, University of Tokyo, 1993 (unpublished).
[21] R.J. Hamers, R.M. Tromp, and J.E. Demuth, Phys. Rev. Lett. **56**, 1972 (1986).
[22] J.E. Northrup, Phys. Rev. Lett. **57**, 154 (1986).
[23] T. Suzuki, Phys. Rev. B **61**, R5117 (2000).
[24] Ph. Avouris and R. Wolkow, Phys. Rev. B **39**, 5091 (1989).
[25] J.C. Slater, J. Chem. Phys. **39**, 3199 (1964).
[26] K. Mochiji and M. Ichikawa, Phys. Rev. B **63**, 115407 (2001).
[27] K. Shudo, T. Sasaki, M. Tanaka, and T. Shirao, Solid State Commun. **127**, 203 (2003).
[28] M. Schülter, J.R. Chelikowsky, S.G. Louie, and M.L. Cohen, Phys. Rev. B **12**, 4200 (1975).
[29] C. Noguez, A.I. Shkrebtii, and R. Del Sole, Surf. Sci. **331–333**, 1349 (1995).
[30] H. Sakamoto and Y. Takakuwa (unpublished).
[31] P. Gupta, P.A. Coon, B.G. Koehler, and S.M. George, Surf. Sci. **249**, 92 (1991).
[32] P. Gupta, P.A. Coon, B.G. Koehler, and S.M. George, J. Chem. Phys. **93**, 2827 (1989).
[33] A. Szabo, P.D. Farrall, and T. Engel, Surf. Sci. **312**, 284 (1994).
[34] R.B. Jackman, R.J. Price, and J.S. Foord, Appl. Surf. Sci. **36**, 296 (1989).
[35] R.B. Jackman, H. Ebert, and J.S. Foord, Surf. Sci. **176**, 183 (1986).
[36] B. Voighländer, M. Kästner, and P. Šmilauer, Phys. Rev. Lett. **81**, 858 (1998).
[37] I.-S. Hwang, M.-S. Ho, and T.-T. Tsong, J. Phys. Chem. Solids **62**, 1655 (2001).
[38] H. Tochihara, W. Shimada, H. Yamamoto, M. Taniguchi, and A. Yamagishi, Jpn. J. Appl. Phys., Part 1 **67**, 1513 (1998).
[39] T. Ishimaru, K. Shimada, T. Hoshino, T. Yamawaki, and I. Ohdomari, Phys. Rev. B **60**, 13 592 (1999).
[40] T. Shirao, K. Shudo, Y. Tanaka, T. Ishikawa, and M. Tanaka, Jpn. J. Appl. Phys., Part 2 **42**, L386 (2003).